GEOPHYSICAL RESEARCH LETTERS, VOL. 23, NO. 13, PAGES 1629-1632, JUNE 15, 1996

A note on the transport of the Brazil Current

Zulema D. Garraffo
Dept. of Applied Physics, Columbia University, and NASA Goddard Institute for Space Studies, New York

Vladimir M. Kamenkovich ,[1]
Lamont-Doherty Earth Observatory of Columbia University, Palisades, New York

Abstract. Stommel's hypothesis on the influence of the thermohaline circulation on the transport of the Brazil Current is illustrated using the product of Semtner and Chervin's model. The velocity distribution along specifically chosen zonal sections is analyzed. A procedure of singling out the thermohaline component of the circulation is suggested and the significance of the component is proved.

Stommel [1965; p. 170] was the first to argue that the relatively low magnitude of the transport of the Brazil Current is due to the influence of the thermohaline component of the general circulation. The purpose of this note is to illustrate this point by using the product of Semtner and Chervin's primitive equation global model [*Semtner,* 1995, a, b; *Stammer et al.,* 1996].

The model is described as POCM_ 4A in *Stammer et al.* [1996]. *Semtner and Chervin* [1992] give the basic model formulation. The model has a resolution of .4 degrees in longitude, latitudinal spacing equal to .4 degrees times the cosine of latitude (average .25 degrees), and 20 vertical levels. Surface winds interpolated from monthly fields from the ECMWF analysis are applied [*Trenberth et al.,* 1989]. The present work is based on the time mean over 3 3/4 years produced by Semtner and Chervin (from April 1986 through December 1989). An analysis of the model in relation to observations can be found in *Stammer et al.* [1996]; the comparison of a previous version of the model with observations for the Brazil Current was presented by *Garzoli et al.* [1992].

Figure 1 shows the transport stream function Ψ for the region between latitudes 4.6°S and 49.2°S, calculated from the model output according to the following formula:

$$\Psi = \int_{\lambda_w}^{\lambda} \left(\int_{-H}^{0} v\, dz \right) a \cos\phi \, d\lambda \qquad (1)$$

where λ is the longitude; ϕ is the latitude; λ_w is the longitude of the western coast; a is the Earth's radius; H is the depth of the ocean; and v is the meridional velocity.

[1] On leave from P. P. Shirshov Institute of Oceanology, the Russian Academy of Sciences, Moscow, Russia.

Paper number 96GL01369
0094-8534/96/96GL-01369$05.00

The Brazil Current is clearly seen on this figure. For the analysis we select five zonal sections: one is located approximately at the source of the current (19.8°S), another one at the latitude of the maximum strength of the current (31.0°S), and the rest at some intermediate latitudes (23.5°S, 26.1°S and 28.9°S). Here we study only the meridional velocity field along these sections, with no explicit analysis of temperature and salinity.

The Sverdrup relation is expressed as:

$$\beta V = curl_z \tau \qquad (2)$$

where β is the latitudinal variation of the Coriolis parameter, $V = \int_{-H}^{0} v\, dz$ is the vertically integrated meridional velocity, and $\rho_0 \tau$ is the wind stress (ρ_0 is the mean density). We define the Sverdrup transport stream function as:

$$\Psi_{Sv}(\lambda, \phi) = -\frac{1}{\beta} \int_{\lambda}^{\lambda_e} (curl_z \tau) a \cos\phi \, d\lambda \qquad (3)$$

where λ_e is the longitude of the eastern coast. This definition implies that Ψ_{Sv} equals zero at the eastern coast. The Sverdrup transport stream function is given in Figure 2 (for the latitude band 4.6°S–35°S).

The meridional velocity along the western part of the zonal sections is shown in Figure 3.

It is useful to check the validity of the Sverdrup relation (2) against the data of Semtner and Chervin's model for our sections (Figure 4). As expected, the

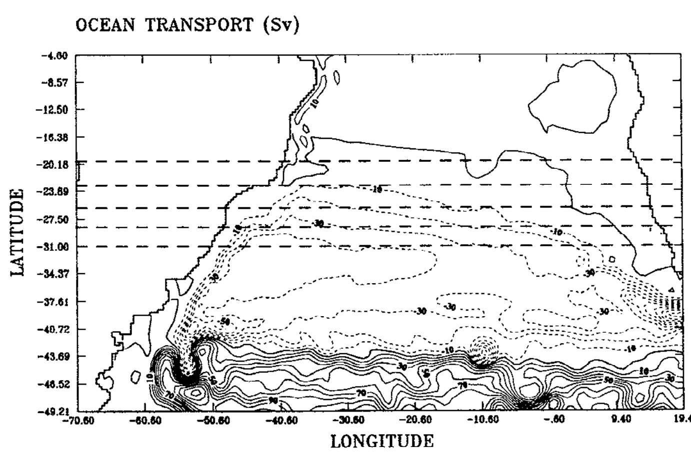

Figure 1. Isolines of the transport stream function according to Semtner and Chervin's model. Contour interval is 10 Sv. The location of five sections selected for the analysis is indicated.

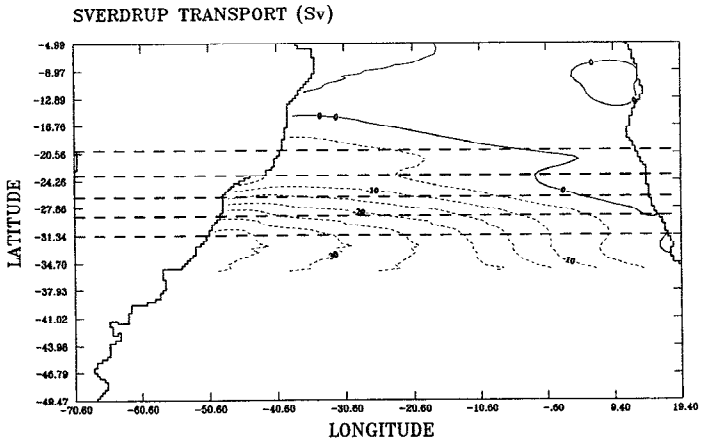

Figure 2. Isolines of the Sverdrup solution (3). Contour interval is 5 Sv. The location of the sections of Figure 1 is indicated.

Sverdrup relation does not hold in the western boundary layer, marked by vertical dashed lines (the boundary between the western boundary region and the interior is marked as "w"). Outside of the western boundary region, the Sverdrup relation holds for the section at 19.8°S, except for local discrepancies at 8°W and at 5°E. Similar deviations occur at 13°W, 10°W and 3°E for the section at 23.5°S. The agreement is also reasonably good for the section at 26.1°S, except for deviations which are of a smaller amplitude than in the previous section but more spread out. At 28.9°S there is a local deviation at 10°W, and noticeable deviations east of this location. For the section at 31.0°S, deviations in the open ocean (away from the eastern and western boundaries) are larger than for the other sections, but still the agreement is satisfactory. In the eastern part of this section the Sverdrup relation is evidently not valid; the deviation is due mainly to upper flows (not shown). From an analysis of instantaneous fields it is quite clear that the current in this region is strongly influenced by eddies shed from the Agulhas Retroflection Current and therefore is governed by high order dynamics. A comparison of the model Agulhas eddies with observations was done by *Garraffo and Garzoli* [1994].

A similar nonuniform character of the validity of the Sverdrup relation was pointed out in both observational [*Schmitz et al.*, 1992] and theoretical [*Bryan et al.*, 1995] studies for the North Atlantic. We can think of the deviations from the Sverdrup relation in the interior of the ocean (away from the western boundary) as being caused by either the existence of bottom flows, or by high order dynamics. The correspondence of discrepancies with bottom flows can be seen in the southwards anomalies near 10°W in all sections, (marked "a" in Figure 4; the sign of the bottom flows is indicated), located in the eastward side of the Mid Atlantic Ridge. Northwards anomalies corresponding with bottom flows (marked "b") are present in the sections at 19.8°S and 23.5°S, and are located in the westward side of ridges. Other bottom flows are marked with their signs in the sections at 23.5°S, 28.9°S and 31.0°S. We assume that they are thermohaline driven (these should be the flows of Antarctic Bottom Water and branches of North Atlantic Deep Water). As is well known, under the influence of bottom topography deep thermohaline flows can

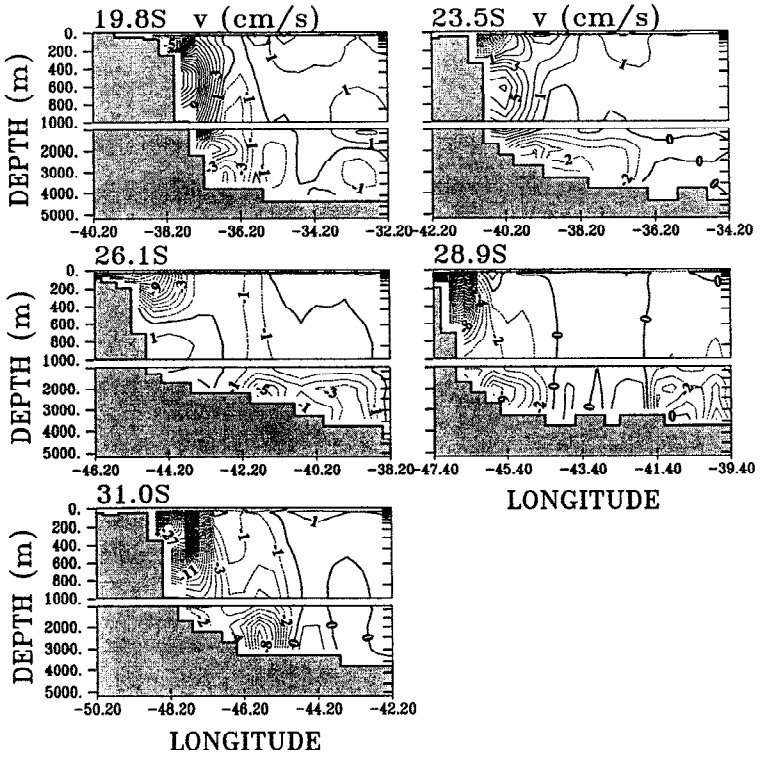

Figure 3. Meridional velocity along the western part of the sections according to Semtner and Chervin's model. Southward velocities are contoured by dashed lines. Contour interval is 1 cm/s. Model level centers are marked on the right hand side of the figure.

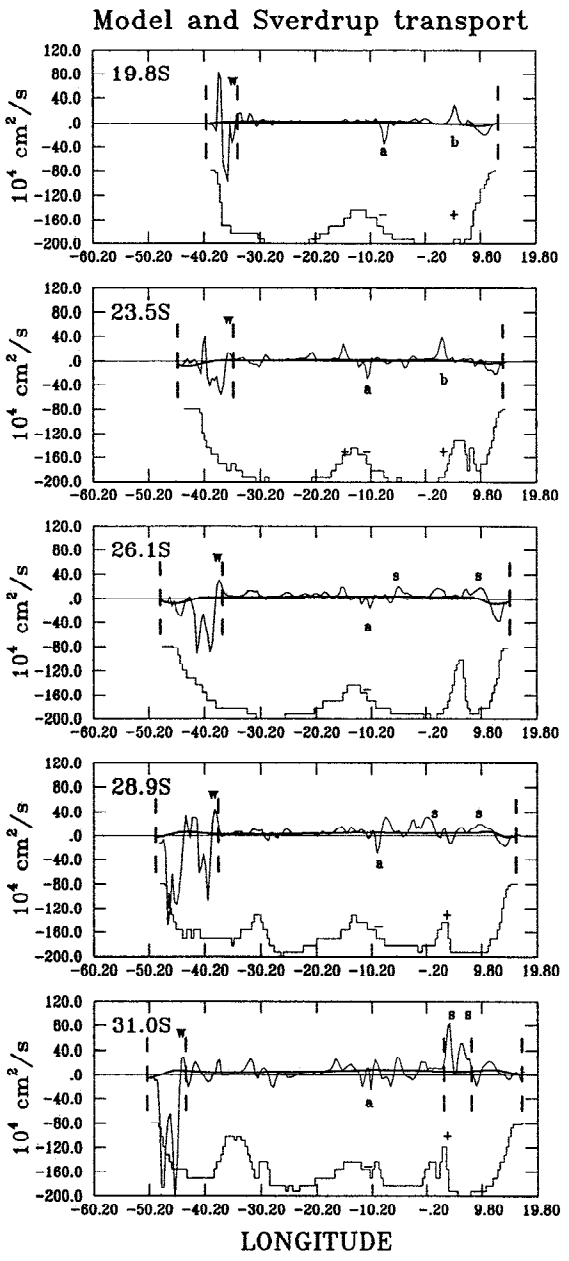

Figure 4. Vertically integrated meridional velocity as a function of longitude for the sections, according to Semtner and Chervin's model (thin lines) and to the Sverdrup relation (2) (thick lines). The vertical dashed lines indicate the coasts and the western boundary layer for all sections, as well as the location of the eastern region for the section at 31°S. "a", "b" mark the correspondence of deviations with bottom flows. Surface flows are marked "s". See text for other notation.

generate noticeable vertical velocities near the bottom that destroy the validity of the Sverdrup relation (2). The largest deviation from the Sverdrup relation due to the high order dynamics of the upper ocean flow occurs within the eastern boundary current for the section at 31.0°S. Northwards upper flows (not shown) are also present in the sections at 28.9°S (as mentioned above, at 0° and 10°E), and at 26.1°S (3°W and 10°E; all marked "s"in Figure 4).

We attribute these discrepancies in the eastern boundary layer to the existence of the thermohaline component as well. The reason is that this current plays a substantial role in closing the global thermohaline cell [*Gordon*, 1986; *Gordon et al.*, 1992].

Our principal objective is to separate the contribution of the wind-driven and thermohaline components to the total meridional transports through the selected sections both in the western boundary layer and in the interior. In observational studies such a separation is based mainly on the investigation of the distribution of the characteristics of water masses (temperature, salinity, oxygen, etc.). Here we consider only the velocity distribution and proceed with the analysis in the following way. First, we break down the whole area into the region near the western coast (western boundary layer) and the rest of the area (the interior of the ocean). Second, to disclose the well-defined current below the level of about 1300 m, we break down the western boundary layer into the upper layer and the lower layer. From the model we obtain the total transports in the western boundary layer (in both upper and lower layers) and in the interior (eastwards of locations "w" in Figure 4). Our analysis is based on the following hypotheses.

1st hypothesis. There is no wind-driven component of the flow in the lower layer of the western boundary region. Figure 3 clearly shows that there is almost no variations in the transport of the flow in the lower layer for the sections, while the wind-stress curl varies substantially: all variations of the transport are confined to the upper layer. We will identify the lower-layer current as North Atlantic Deep Water (NADW) flow, and the upper-layer flow as the Brazil Current. With this definition, we are including in the "Brazil Current" the northward flowing Intermediate Water (Figure 3).

2nd hypothesis. Based on the analysis of the validity of the Sverdrup relation, we assume that the Sverdrup transport $\psi_{Sv}(\lambda_w, \phi)$, (eq. 3) gives the total transport of the wind-driven component in the interior of the ocean. The remainder of the total transport in the interior is due to the thermohaline component.

Now we can decompose the total transport in the interior of the ocean into the wind-driven and thermohaline-driven components (Table 1). To show the sensitivity of the method, slightly different ways of separating boundary layer and interior flows are presented: in Case 1 the separation between the boundary layer and the interior follows the exact contours of the flows, and the boundary between western upper and lower flows is at 1335m; in Case 2 the separation between western boundary and interior follows the vertical line "w" (Figure 4) with the same horizontal boundary; in Case 3 the boundary between the western upper and lower flows is taken at 985m, with the same vertical boundary as in Case 1. Case 3 is shown for sensitivity estimates. We consider Cases 1 and 2 to be more adequate.

Since the total transport of the thermohaline circulation across a whole section is equal to zero, we can immediately find the transports of the thermohaline component of the Brazil Current; this component seems to be the northwards flowing Intermediate Water (Table 1). Then we obtain the wind-driven component of the Brazil Current (Table 1).

Table 1.

Section	Total	TH Bnd. Layer	W	Total	TH Interior	W
Case 1	Upper (Brazil)					
19.8S	5.7	12.2	-6.5	8.3	1.8	6.5
23.5S	6.3	12.8	-6.5	10.4	3.9	6.5
26.1S	-7.2	5.8	-13.	26.6	13.6	13.
28.9S	-17.	7.	-24.	35.8	11.8	24.
31.0S	-27.1	7.9	-35.	46.	11.	35.
	Lower (NADW)					
19.8S	-14.	-14.	0			
23.5S	-16.7	-16.7	0			
26.1S	-19.4	-19.4	0			
28.9S	-18.8	-18.8	0			
31.0S	-18.9	-18.9	0			
Case 2	Upper (Brazil)					
19.8S	6.8	13.3	-6.5	6.8	.3	6.5
23.5S	5.6	12.1	-6.5	10.4	3.9	6.5
26.1S	-7.3	5.7	-13.	26.1	13.1	13.
28.9S	-17.8	6.2	-24.	35.2	11.2	24.
31.0S	-27.	8.	-35.	45.	10.	35.
	Lower (NADW)					
19.8S	-13.6	-13.6	0			
23.5S	-16.	-16.	0			
26.1S	-18.8	-18.8	0			
28.9S	-17.4	-17.4	0			
31.0S	-18.	-18.	0			
Case 3	Upper (Brazil)					
19.8S	6.7	13.2	-6.5	8.3	1.8	6.5
23.5S	4.3	10.8	-6.5	12.6	6.1	6.5
26.1S	-8.2	4.8	-13.	28.5	15.5	13.
28.9S	-15.6	8.4	-24.	36.4	12.4	24.
31.0S	-24.2	10.8	-35.	46.	11.	35.
	Lower (NADW)					
19.8S	-15.	-15.	0			
23.5S	-16.9	-16.9	0			
26.1S	-20.3	-20.3	0			
28.9S	-20.8	-20.8	0			
31.0S	-21.8	-21.8	0			

Table 1. Transport of the thermohaline (TH) and wind-driven (W) components of the Brazil Current, North Atlantic Deep Water flow, and the interior motion for the selected sections in Sv. Positive numbers indicate northward transport. Cases 1, 2 and 3 are described in the text. The lower layer flow across the whole Atlantic ranges from -17.8 Sv to -18.4 Sv for all the sections.

From Table 1 we see that the thermohaline component contributes substantially to the total transport of the Brazil Current (*e.g.* 30% of the total at 31.0°S); this is in full agreement with Stommel's hypothesis.

We note that there are two values of the transport of the thermohaline component of the upper western boundary flow: 6–8Sv for 26.1°S to 31.0°S and 12–13Sv for 19.8°S to 23.5°S, for Case 1. We can interpret this results as follows: the part of the thermohaline circulation in the interior of the southern sections (which starts with the Agulhas-Benguela system), migrates to the west where it merges with the western boundary in the northern sections. The upper western boundary current changes sign, being southwards for the southern sections and northwards for the two northern sections.

We can conclude that the importance of the thermohaline circulation in the western South Atlantic implies that any relevant regional model of the Brazil Current has somehow to take into account the thermohaline component of the current. The difficulty is that the thermohaline component is generated beyond the region of the subtropical gyre.

Acknowledgments

The authors gratefully acknowledge discussions with A. Gordon and S. Garzoli, and the comments of two anonymous reviewers. We are also very grateful to A. Semtner for providing output data of the numerical experiments. Z. Garraffo was funded through the NASA / Columbia University cooperative agreement NCC5-34. V. Kamenkovich was supported by grant NSF OCE 94-01950. This is a Lamont-Doherty Earth Observatory Contribution No. 5503.

References

Bryan, F. O., C. W. Boning, and W. R. Holland, On the midlatitude circulation in a high-resolution model of the North Atlantic, *J. Phys. Oceanogr.*, 25, 289–305, 1995.

Garraffo, Z. D., and S. L. Garzoli, Mass, heat and salt exchanges between the Indian Ocean and the Atlantic Ocean from a Global Ocean General Circulation model, IAPSO Workshop, Cape Town, South Africa, March 28-April 1, 1994.

Garzoli, S. L, Z. Garraffo, G. Podesta, and O. Brown, Analysis of a general circulation model product. 1. Frontal systems in the Brazil/Malvinas and Kuroshio/Oyashio Regions, *J. Geophys. Res.*, *97*, 20,117–20,138, 1992.

Gordon, A., Interocean exchange of thermocline water. *J. Geophys. Res.*, *91C*, 5037–5046, 1986.

Gordon, A., R. F. Weiss, W. M. Smethie, Jr, and M. J. Warner, Thermocline and Intermediate Water communication between the South Atlantic and Indian Oceans, *J. Geophys. Res.*, *97C*, 7223–7240, 1992.

Schmitz, W. J., Jr., J. D. Thompson, and J. R. Luyten, The Sverdrup circulation for the Atlantic along 24°N. *J. Geophys. Res.*, *97*, 7251–7256, 1992.

Semtner, A.J., Very high-resolution estimates of global ocean circulation, suitable for carbon-cycle modeling. *Proceedings of the Snowmass Global Change Institute on the Global Carb on Cycle, Office of Interdisciplinary Earth Studies, Boulder*, 1995a.

Semtner, A. J., Modeling ocean circulation. *Science*, 269, 1379, 1995b.

Semtner, A. J. and R. M. Chervin, Ocean general circulation from a global eddy-resolving model. *J. Geophys. Res.*, 97, 5493–5550, 1992.

Stammer, D., R. Tokmakian, A. Semtner and C. Wunsch, How well does a 1/4° global circulation model simulate large-scale oceanic observations? Submitted to *J. Geophys. Res.*, 1996.

Stommel, H., *The Gulf Stream. A physical and dynamical description*, 2nd Ed., University of California Press, Berkeley, 248pp., 1965.

Trenberth, K.E., J.G. Olson, and W.G. Large, A global ocean wind stress climatology based ECMWF analyses, *NCAR/TN-338+STR*, NCAR Tech. Note, NCAR, 93 pp., 1989.

Z. D. Garraffo, Dept. of Applied Physics, Columbia University, and NASA Goddard Institute for Space Studies, 2880 Broadway, New York, N.Y. 10025.

V. M. Kamenkovich, Lamont-Doherty Earth Observatory of Columbia University, Palisades, NY 10964.

(received March 1, 1996; accepted April 2, 1996.)